Ultralow-dose chest computed tomography for pulmonary nodule detection: First performance evaluation of single energy scanning with spectral shaping

Gordic, Sonja ; Morsbach, Fabian ; Schmidt, Bernhard ; Allmendinger, Thomas ; Flohr, Thomas ; Husarik, Daniela ; Baumueller, Stephan ; Raupach, Rainer ; Stolzmann, Paul ; Leschka, Sebastian ; Frauenfelder, Thomas ; Alkadhi, Hatem

Abstract: PURPOSE: The purpose of this study was to evaluate the image quality and sensitivity of ultralow radiation dose single-energy computed tomography (CT) with tin filtration for spectral shaping and iterative reconstructions for the detection of pulmonary nodules in a phantom setting. METHODS: Single-energy CT was performed using third-generation dual-source CT (SOMATOM Force; 2 × 192 slices) at 70 kVp, 100 kVp with tin filtration (100Sn kVp), and 150Sn kV with tube current-time product adjustments resulting in standard dose (CT volume dose index, 3.1 mGy/effective dose, 1.3 mSv at a scan length of 30 cm), 1/10th dose level (0.3 mGy/0.13 mSv), and 1/20th dose level (0.15 mGy/0.06 mSv). An anthropomorphic chest phantom simulating an intermediate-sized adult with randomly distributed solid pulmonary nodules of various sizes (2-10 mm; attenuation, 75 HU at 120 kVp) was used. Images were reconstructed with advanced model-based iterative reconstruction (ADMIRE; strength levels 3 and 5) and were compared with those acquired with second-generation dual-source CT at 120 kVp (reconstructed with filtered back projection) and sinogram-affirmed iterative reconstruction (strength level 3) at the lowest possible dose at 120 kVp (CT volume dose index, 0.28 mGy). One blinded reader measured image noise, and 2 blinded, independent readers determined overall image quality on a 5-grade scale (1 = nondiagnostic to 5 = excellent) and marked nodule localization with confidence rates on a 5-grade scale (1 = unsure to 5 = high confidence). The constructional drawing of the phantom served as reference standard for calculation of sensitivity. Two patients were included, for proof of concept, who were scanned with the 100Sn kVp protocol at the 1/10th and 1/20th dose level. RESULTS: Image noise was highest in the images acquired with second-generation dual-source CT and reconstructed with filtered back projection. At both the 1/10th and 1/20th dose levels, image noise at a tube voltage of 100Sn kVp was significantly lower than in the 70 kVp and 150Sn kV data sets (ADMIRE 3, $P < 0.01$; ADMIRE 5, $P < 0.05$). Sensitivity of nodule detection was lowest in images acquired with second-generation dual-source CT at 120 kVp and the lowest possible dose. Protocols at 100Sn kVp and ADMIRE 5 showed highest sensitivity at the 1/10th and 1/20th dose levels. Highest numbers of false-positives occurred in second-generation dual-source CT images (range, 12-15), whereas lowest numbers occurred in the 1/10th and 1/20th dose data sets acquired with third-generation dual-source CT at 100Sn kVp and reconstructed with ADMIRE strength levels 3 and 5 (total of 1 and 0 false-positives, respectively). Diagnostic confidence at 100Sn kVp was significantly higher than at 70 kVp or 150Sn kV (ADMIRE 3, $P < 0.05$; ADMIRE 5, $P < 0.01$) at both the 1/10th and 1/20th dose levels. Images of the 2 patients scanned with 100Sn kVp at the 1/10th and 1/20th dose levels were of diagnostic quality. CONCLUSIONS: Our study suggests that chest CT for the detection of pulmonary nodules can be performed with third-generation dual-source CT producing high image quality, sensitivity, and diagnostic confidence at a very low effective radiation dose of 0.06 mSv when using a single-energy protocol at 100 kVp with spectral shaping and when using advanced iterative reconstruction techniques.

DOI: https://doi.org/10.1097/RLI.0000000000000037

Ultralow-Dose Chest Computed Tomography for Pulmonary Nodule Detection

First Performance Evaluation of Single Energy Scanning With Spectral Shaping

Sonja Gordic, MD, Fabian Morsbach, MD,* Bernhard Schmidt, PhD,†‡ Thomas Allmendinger, PhD,† Thomas Flohr, PhD,†§ Daniela Husarik, MD,* Stephan Baumueller, MD,* Rainer Raupach, PhD,† Paul Stolzmann, MD,* Sebastian Leschka, MD,|| Thomas Frauenfelder, MD,* and Hatem Alkadhi, MD, MPH, EBCR**

Purpose: The purpose of this study was to evaluate the image quality and sensitivity of ultralow radiation dose single-energy computed tomography (CT) with tin filtration for spectral shaping and iterative reconstructions for the detection of pulmonary nodules in a phantom setting.

Methods: Single-energy CT was performed using third-generation dual-source CT (SOMATOM Force; 2 × 192 slices) at 70 kVp, 100 kVp with tin filtration (100Sn kVp), and 150Sn kV with tube current-time product adjustments resulting in standard dose (CT volume dose index, 3.1 mGy/effective dose, 1.3 mSv at a scan length of 30 cm), 1/10th dose level (0.3 mGy/0.13 mSv), and 1/20th dose level (0.15 mGy/0.06 mSv). An anthropomorphic chest phantom simulating an intermediate-sized adult with randomly distributed solid pulmonary nodules of various sizes (2–10 mm; attenuation, 75 HU at 120 kVp) was used. Images were reconstructed with advanced model-based iterative reconstruction (ADMIRE; strength levels 3 and 5) and were compared with those acquired with second-generation dual-source CT at 120 kVp (reconstructed with filtered back projection) and sinogram-affirmed iterative reconstruction (strength level 3) at the lowest possible dose at 120 kVp (CT volume dose index, 0.28 mGy). One blinded reader measured image noise, and 2 blinded, independent readers determined overall image quality on a 5-grade scale (1 = nondiagnostic to 5 = excellent) and marked nodule localization with confidence rates on a 5-grade scale (1 = unsure to 5 = high confidence). The constructional drawing of the phantom served as reference standard for calculation of sensitivity. Two patients were included, for proof of concept, who were scanned with the 100Sn kVp protocol at the 1/10th and 1/20th dose level.

Results: Image noise was highest in the images acquired with second-generation dual-source CT and reconstructed with filtered back projection. At both the 1/10th and 1/20th dose levels, image noise at a tube voltage of 100Sn kVp was significantly lower than in the 70 kVp and 150Sn kV data sets (ADMIRE 3, $P < 0.01$; ADMIRE 5, $P < 0.05$). Sensitivity of nodule detection was lowest in images acquired with second-generation dual-source CT at 120 kVp and the lowest possible dose. Protocols at 100Sn kVp and ADMIRE 5 showed highest sensitivity at the 1/10th and 1/20th dose levels. Highest numbers of false-positives occurred in second-generation dual-source CT images (range, 12–15), whereas lowest numbers occurred in the 1/10th and 1/20th dose data sets acquired with third-generation dual-source CT at 100Sn kVp and reconstructed with ADMIRE strength levels 3 and 5 (total of 1 and 0 false-positives, respectively). Diagnostic confidence at 100Sn kVp was significantly higher than at 70 kVp or 150Sn kV (ADMIRE 3, $P < 0.05$; ADMIRE 5, $P < 0.01$) at both the 1/10th and 1/20th dose levels. Images of the 2 patients scanned with 100Sn kVp at the 1/10th and 1/20th dose levels were of diagnostic quality.

Conclusions: Our study suggests that chest CT for the detection of pulmonary nodules can be performed with third-generation dual-source CT producing high image quality, sensitivity, and diagnostic confidence at a very low effective radiation dose of 0.06 mSv when using a single-energy protocol at 100 kVp with spectral shaping and when using advanced iterative reconstruction techniques.

Key Words: computed tomography, image reconstruction, lung, radiation dosage, low dose

(*Invest Radiol* 2014;49: 465–473)

Ongoing debates about the assumed radiation-associated risk of cancer development from ionizing radiation has urged the radiologic community to lower the dose of each computed tomography (CT) study to a level that is "as low as reasonably achievable" (the so-called ALARA principle). This holds particularly true for the cumulative dose associated with repetitive CT studies or for screening purposes. Various strategies exist for lowering the radiation dose of CT. These include lowering of the tube voltage and/or tube current, automated exposure control, selective in-plane shielding, and iterative reconstructions (IRs).[1–13]

Regarding chest imaging, a recent multicenter trial (National Lung Screening Trial) on lung cancer screening showed a reduced mortality from lung cancer when using a protocol with a radiation dose of 1.5 mSv.[14] In this trial, patients underwent 3 screening studies with CT at 1-year intervals, indicating a considerable cumulative radiation dose when assuming a lung cancer screening program with CT in the general population.

Recently, a third-generation dual-source CT was introduced. In contrast to second-generation dual-source CT, this machine can be optionally operated with 2 selective photon shields (Dual Selective Photon Shield II; Siemens Healthcare, Forchheim, Germany), represented by a tin filter (TF) mounted in front of both x-ray tubes, to allow also for single-energy scanning with TF. In dual-energy CT, the TF has proven to increase the mean photon energy of the 140-kVp spectrum, thereby on the one hand improving the separation of the 2 energy spectra and thus allowing for an improved dual-energy postprocessing. On the other hand, it was shown that spectral shaping of the high-kVp beam leads to a more efficient x-ray beam, allowing for a reduction in radiation dose.[15]

In addition, the third-generation dual-source CT includes a new generation of IR, that is, advanced model-based IR (ADMIRE), which combines in an iterative approach the statistical data modeling

Received for publication November 15, 2013; and accepted for publication, after revision, December 17, 2013.

From the *Institute for Diagnostic and Interventional Radiology, University Hospital Zurich, Switzerland; †Computed Tomography Division, Siemens Healthcare, Forchheim, ‡University of Erlangen-Nuremberg, Erlangen; §University of Tübingen, Tübingen, Germany; and ||Institute of Radiology, Kantonsspital St. Gallen, Switzerland.

Conflicts of interest and sources of funding: none declared.

Reprints: Hatem Alkadhi, MD, MPH, EBCR, Institute of Diagnostic and Interventional Radiology, University Hospital Zurich, Raemistrasse 100, CH-8091 Zurich, Switzerland. E-mail: hatem.alkadhi@usz.ch.

ISSN: 0020-9996/14/4907–0465

in the raw data domain and a model-based noise detection in the image domain.

The purpose of this study was to evaluate the image quality, sensitivity, and diagnostic confidence of ultralow radiation dose single-energy CT with spectral shaping and reconstructions using ADMIRE for the detection of pulmonary nodules in a phantom model.

MATERIALS AND METHODS

Phantom

We designed a chest phantom that was custom-made by a specialized manufacturer (Quality Assurance in Radiology and Medicine, Moehrendorf, Germany). The anthropomorphic chest phantom (serial number B13065; Quality Assurance in Radiology and Medicine) of adult size (lateral diameter, 35 cm; anteroposterior diameter, 25 cm; extension ring of 2.5 cm thickness) contains 18 solid pulmonary nodules of various sizes (2–10 mm; attenuation, 75 HU at 120 kVp). Each of these nodules is surrounded by cork granulate material with an air equivalent CT number (−800 HU at 120 kVp) simulating lung parenchyma. The chest phantom consists of materials made from resin and additives, specifically including calcium carbonate, magnesium oxide, hydroxyapatite, and microspheres representing solid, noncalcified pulmonary nodules, soft tissue, lung, and bone equivalent structures, respectively, to simulate tissue-equivalent material for all investigated x-ray spectra.

CT Scan Protocol

All data, except of those at a tube voltage of 120 kVp (see below), were acquired on a third-generation dual-source CT machine (SOMATOM Force; Siemens Healthcare) equipped with an integrated high-resolution circuit detector (Stellar Technology; Siemens).[16] The phantom was scanned with a collimation of 96 × 0.6 mm and a slice acquisition of 192 × 0.6 mm by means of a z-flying focal spot, gantry rotation time of 0.25 seconds, and pitch of 1.2. Single-energy data sets were acquired at tube voltages of 70 kVp and 100 and 150 kVp, whereas TF was used at 100 and 150Sn kV. As demonstrated in Figure 1, the TF leads to a substantial hardening of the spectra and, thus, to more narrow spectra with less quanta at low energies. Reference tube current-time products were adjusted to obtain 3 defined radiation dose levels (CT volume dose index [$CTDI_{vol}$]) for each tube voltage:

- standard dose, 3.1 mGy: 70 kVp/335 ref. mAs, and 150Sn kV/136 ref. mAs;
- 1/10th dose, 0.31 mGy: 70 kVp/33 ref. mAs, 100Sn kVp/110 ref. mAs, and 150Sn kV/13 ref. mAs; and
- 1/20th dose, 0.15 mGy: 70 kVp/13 ref. mAs, 100Sn kVp/46 ref. mAs, and 150Sn kV/5 ref. mAs.

Images at the standard dose level of 3.1 mGy could not be obtained at the tube voltage level of 100 kVp with TF because with spectral shaping, the tube power was not sufficiently high for allowing the necessary increase in tube current. Scans included the entire phantom with a constant scan length in the z-axis of 30 cm, hereby simulating the craniocaudal distance of an adult lung. Scan duration was 3 seconds.

The single-energy data set acquired at 120 kVp was obtained on a second-generation dual-source CT machine (SOMATOM Definition Flash; Siemens Healthcare) equipped with the same detector.[16] Protocol parameters were as follows: collimation, 64 × 0.6 mm; slice acquisition, 128 × 0.6 mm by means of a z-flying focal spot; and gantry rotation time, 0.28 seconds. At 120 kVp, the lowest possible quality reference tube current-time product of 4 mAs was used, resulting in a $CTDI_{vol}$ of 0.28 mGy.

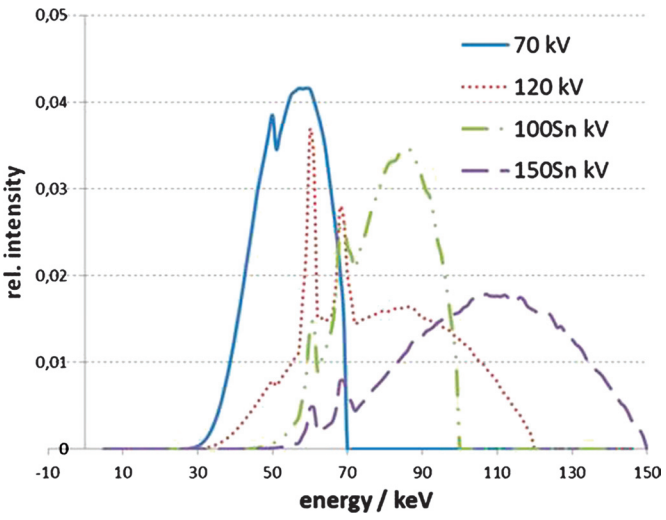

FIGURE 1. Graph illustrating the 70- and 120-kVp spectrum without and the 100- and 150-kVp spectrum with spectral shaping by use of a tin filter (100 and 150Sn kV, respectively). The tin filter reduces dose by blocking low-energy photons out of the x-ray tube spectrum.

Data Reconstruction

All CT images, except the data set acquired with second-generation dual-source CT, were reconstructed with ADMIRE at strength levels of 3 and 5 and using a slice thickness of 2 mm, an increment of 1.6 mm, and a sharp tissue convolution kernel (Br64). The reconstructed field of view (FoV) was 350 mm and the image matrix was 512 × 512 pixels.

The images acquired with second-generation dual-source CT at 120 kVp were reconstructed with filtered back projection (FBP) and sinogram-affirmed IR (SAFIRE)[13] at a strength level of 3 using a slice thickness of 2 mm, an increment of 1.6 mm, and a sharp tissue convolution kernel (B70f for FBP and I70f for SAFIRE). The reconstructed FoV was 350 mm and the image matrix was 512 × 512 pixels.

Subsequent analyses were performed using a picture archiving and communication system workstation on a high-definition liquid crystal display monitor (BARCO; Medical Imaging Systems, Kortrijk, Belgium) using Impax (Version 6.4.0.4551; Agfa-Gevaert, Mortsel, Belgium).

Advanced IR

Iterative reconstruction comprises statistical weighting (statistical modeling in raw data domain) followed by back projection, application of statistical model in image domain (regularization), and forward projection using an adequate system model. The resulting pseudo raw data are compared with the measurement data, that is, subtracted, and reinserted into the loop afterward (Fig. 2). To enable routine applicability and better adaptation to the clinical image quality needs, ADMIRE incorporates 3 substantial modifications compared with statistical IR.

1. Advanced model-based IR uses a weighted FBP in the loop. Mathematically, this corresponds to a preconditioning filter,[17] which accelerates convergence, particularly regarding the removal of artifacts based on geometrically nonexact reconstruction operators such as noniterative FBP.
2. Advanced model-based IR reconstruction starts with up to 2 iterations to remove geometric imperfections such as cone-beam artifacts (loop A). Only a very small number of iterations are necessary here because of preconditioning. Subsequently, iterations

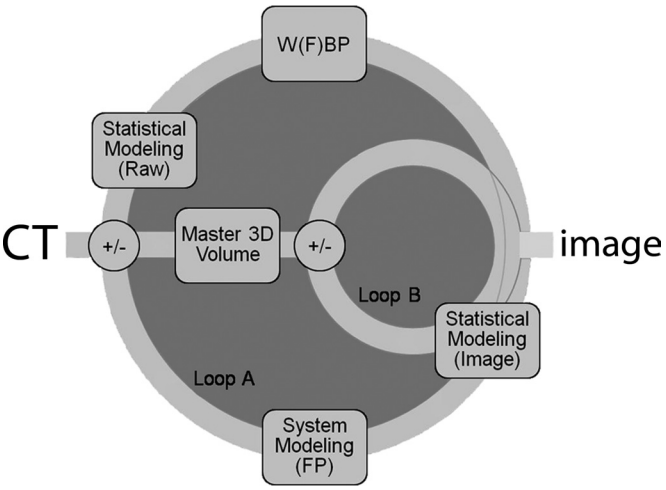

FIGURE 2. Scheme of the ADMIRE algorithm.

in image domain (loop B) are performed to finalize the statistical optimization, that is, reaching a target noise reduction level that depends on the selected ADMIRE strength level.

3. The used statistical modeling for ADMIRE performs a local signal-to-noise ratio analysis to decompose data into "information" and "noise" according to the model. The consecutive comparison with the master 3-dimensional volume can be interpreted as a validation of this assumption. Compared with SAFIRE,[13,18] the analysis incorporates not only nearest-neighbor data but also a larger neighborhood on an anatomically reasonable length scale. Parameters of the model are set depending on the selected reconstruction algorithms (kernels) that are assigned to clinical applications.

The edge properties of ADMIRE are reflected by the modulation transfer function determined by measurements of the edge spread function.[19] This is done by differentiation of the edge profile function measured in the image and subsequent Fourier transformation, resulting in the final modulation transfer function. The edge function for conventional weighted FBP and for ADMIRE at strength levels from 1 to 5 are shown in Figure 3.

Radiation Dose

The radiation dose parameters $CTDI_{vol}$ and dose-length product (DLP) were taken from the electronically logged protocol from each CT study. The effective radiation dose of chest CT was calculated by multiplying the DLP with a conversion coefficient k of 0.014 mSv/mGy cm.[20]

CT Data Analysis

Image Quality

The reconstructed transverse images were presented to 2 independent and blinded readers (each with 3 years of experience in chest CT) in a random distribution. Readers were allowed to modify the window width and level after the initial presentation with a lung tissue window preset (window level, −600 HU; width, 1200 HU). Overall image quality was rated on a modified 5-point Likert scale previously shown[10]: 1, nondiagnostic image quality, strong artifacts, insufficient for diagnostic purposes score; 2, severe blurring with uncertainty about the evaluation; 3, moderate blurring with restricted assessment; 4, slight blurring with unrestricted diagnostic image evaluation possible; and 5, excellent image quality, no artifacts. An image quality with scores of 3 to 5 was considered diagnostic.

Image Noise

One other blinded reader (with 4 years of experience in CT chest imaging) not involved in subjective image quality grading measured image noise by placing a region of interest (ROI) in the center of the phantom (simulating the mediastinum) in a homogenous area representing the central scan-FoV. The ROI size was fixed at 430 mm^2. Mean image noise was defined as the average of the standard deviation of the attenuation in 5 consecutive ROI measurements at different slice positions.

Detection of Pulmonary Nodules

The 2 blinded and independent readers who analyzed the overall image quality also evaluated the number of pulmonary nodules and the diagnostic confidence for each nodule on a modified 5-point Likert scale as previously shown[21]: 1, unsure if true finding; 2, low diagnostic confidence with marginally delineated nodule; 3, intermediate diagnostic confidence with moderately delineated module; 4, high diagnostic confidence with slightly blurred edges of the nodule; and 5, high diagnostic confidence with no blurring of nodule edges.

A total of 18 data sets were reviewed in 2 separate reading sessions separated by 2 weeks and in a random order. Within each data set, the images were presented to the readers in varied order to avoid recall bias on the location of the nodules.

Patients

Two consecutive patients (51-year-old man and 42-year-old woman, respectively), who were referred to our department for nonenhanced chest CT and who were scanned with third-generation dual-source CT using a protocol with 100 kVp and spectral shaping at 1/10th and 1/20th doses, were included in this study for demonstrating the feasibility of the protocol in vivo. The quality reference tube current-time product was set at 96 mAs (114 eff. mAs using CareDose4D; Siemens) for the 1/10th dose and at 45 mAs (41 eff. mAs) for the 1/20th dose protocol.

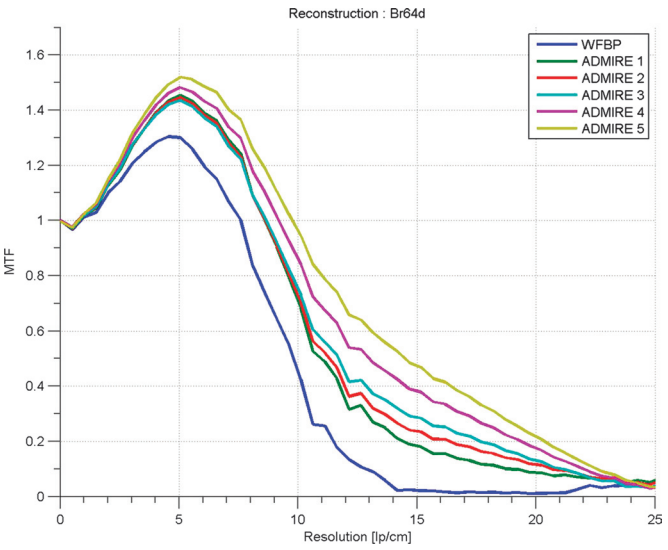

FIGURE 3. Modulation transfer functions of conventional weighted FBP (WFBP) and ADMIRE for all 5 strength levels demonstrating the increase in sharpness because of ADMIRE reconstruction.

TABLE 1. Radiation Dose Parameters of the Protocols With Third-Generation Dual-Source CT

	Standard Dose Protocol	1/10th Dose Protocol	1/20th Dose Protocol
$CTDI_{vol}$, mGy	3.1	0.31	0.15
Scan length, cm	30	30	30
DLP, mGy cm	93	9.3	4.5
ED, mSv	1.30	0.13	0.06

CT indicates computed tomography; $CTDI_{vol}$, CT volume dose index; DLP, dose-length product; ED, effective dose.

Statistical Analysis

Continuous variables were expressed as mean ± SD, and categorical variables were expressed as frequencies or percentages. To determine the interobserver agreement for image quality and diagnostic confidence, the intraclass correlation coefficient (ICC) was calculated for each pair of variables. According to Landis and Koch, ICC values of 0.61 to 0.80 were interpreted as substantial, and 0.81 to 1.00, as excellent agreement.[22]

The Friedman analysis of variance was used to test for significant differences in image noise among the different tube voltage levels. Univariate analysis was performed with the Wilcoxon rank test for evaluating for significant pairwise differences in image noise and diagnostic confidence among the reconstruction algorithms. The Kendall test was used to compare the diagnostic confidence for pulmonary nodule detection between the various tube voltages (ie, 70 kVp, 100Sn kVp, and 150Sn kV). Multivariate analysis was performed with a general linear model for assessing independent predictors (ie, dose, tube voltage, and reconstruction algorithm) of sensitivity and image noise.

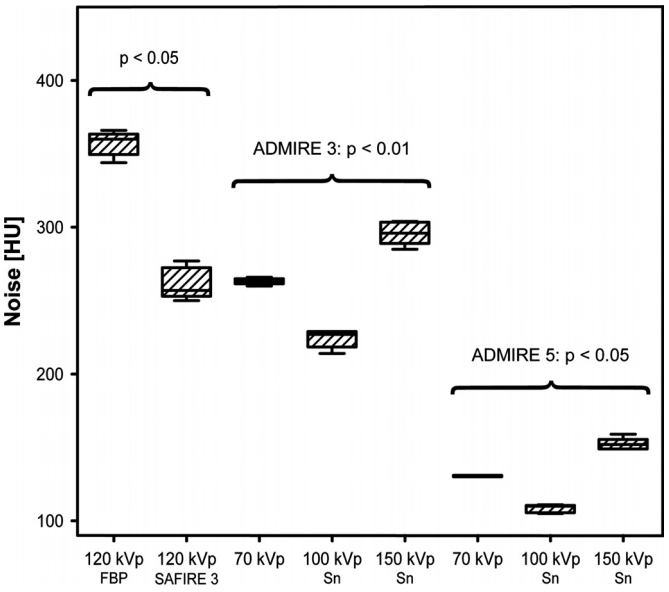

FIGURE 4. Image noise distributions among protocols reconstructed with FBP, SAFIRE, and ADMIRE 3 and 5. At the 1/20th standard dose (SD) level, the protocol with 100Sn kVp was associated with the lowest image noise. Overall, ADMIRE 5 further reduced image noise as compared with ADMIRE 3.

Sensitivity was calculated comparing the readers' marks on the evaluation sheets with the localization of the pulmonary nodules using the constructional drawing of the phantom. Sensitivity was determined along with 95% confidence intervals. In an intent-to-diagnose approach, all data sets were included into the analysis of sensitivity, even if the image quality was considered nondiagnostic.

TABLE 2. Image Noise and Subjective Image Quality for all CT Protocols

				Subjective Image Quality	
CT Scanner	**Protocol**	**Reconstruction**	**Image Noise**	**Reader 1**	**Reader 2**
Second-generation dual-source CT	120 kVp	FBP	357 (344–366)	2	1
	120 kVp	SAFIRE 3	263 (256–277)	2	1
Third-generation dual-source CT	SD 70 kVp	ADMIRE 3	66 (66–67)	5	5
	SD 150Sn kV		57 (55–59)	5	5
	SD 70 kVp	ADMIRE 5	31 (31–32)	5	5
	SD 150Sn kV		27 (26–28)	5	5
	1/10th SD 70 kVp	ADMIRE 3	200 (199–202)	4	3
	1/10th SD 100Sn kVp		156 (151–159)	5	4
	1/10th SD 150Sn kV		188 (176–197)	4	3
	1/10th SD 70 kVp	ADMIRE 5	96 (95–97)	4	3
	1/10th SD 100Sn kVp		74 (72–75)	5	5
	1/10th SD 150Sn kV		93 (89–97)	4	4
	1/20th SD 70 kVp	ADMIRE 3	263 (260–266)	3	2
	1/20th SD 100Sn kVp		224 (214–229)	4	3
	1/20th SD 150Sn kV		294 (285–304)	3	3
	1/20th SD 70 kVp	ADMIRE 5	131 (130–131)	4	3
	1/20th SD 100Sn kVp		109 (105–111)	4	4
	1/20th SD 150Sn kV		152 (149–159)	3	4

Image quality was rated on a 5-point scale (1 = bad, to 5 = excellent). Ranges are displayed in parentheses.

CT indicates computed tomography; SD, standard radiation dose; FBP, filtered back projection; SAFIRE, sinogram-affirmed iterative reconstruction; ADMIRE, advanced model-based iterative reconstruction.

All statistical analyses were conducted using commercially available software (SPSS, release 21.0; SPSS, Chicago, IL, USA). A 2-tailed P value < 0.05 was considered to indicate statistical significance.

RESULTS

Computed tomography and data reconstructions with FBP, SAFIRE 3, and ADMIRE 3 and 5 were feasible without problems, giving rise to a total of 18 phantom and 4 patient data sets for analysis. Time for reconstruction of an image data set was similar for ADMIRE 3 and ADMIRE 5 (15.8 ± 0.2 seconds).

Estimated Radiation Doses

Radiation dose parameters of the different protocols are summarized in Table 1. The effective radiation dose of the standard dose protocol was 1.30 mSv, the effective radiation dose at 1/10th of the standard dose was 0.13 mSv, and the effective radiation dose at 1/20th of the standard dose was 0.06 mSv.

Image Quality

There was a good interobserver agreement for ratings of overall image quality with ADMIRE strength level 3 (ICC = 0.74) and ADMIRE strength level 5 (ICC = 0.72).

Overall image quality was rated by readers to be worst for the protocol acquired with second-generation dual-source CT at a tube voltage of 120 kVp and lowest possible mAs and with images reconstructed with FBP and SAFIRE 3 (Table 2). Image quality of all standard dose protocols regardless of tube voltage and reconstruction algorithm was rated highest by both readers. Within the 1/10th and 1/20th radiation dose levels, image quality was highest for the 100Sn kVp data sets as compared with 70 kVp and 150Sn kV at similar dose levels (Table 2).

TABLE 3. Sensitivity for Lung Nodule Detection for all Protocols

CT Scanner	Protocol	Reader	TP	FP	FN	Sensitivity (95% CI)
Second-generation dual-source CT	120 kVp FBP	R1	14	15	4	77% (55%–91%)
		R2	15	13	3	83% (61%–94%)
	120 kVp SAFIRE 3	R1	15	12	3	83.3% (61%–94%)
		R2	16	12	2	88.9% (67%–97%)
Third-generation dual-source CT	SD, 70 kVp, ADMIRE 3	R1	17	0	1	94% (74%–99%)
		R2	16	1	2	89% (67%–97%)
	SD, 150Sn kV, ADMIRE 3	R1	17	0	1	94% (74%–99%)
		R2	18	2	0	100% (82%–100%)
	SD, 70 kVp, ADMIRE 5	R1	17	0	1	94% (74%–99%)
		R2	17	0	1	94% (74%–99%)
	SD, 150Sn kV, ADMIRE 5	R1	17	0	1	94% (74%–99%)
		R2	18	0	0	100% (82%–100%)
	1/10th SD, 70 kVp, ADMIRE 3	R1	17	1	1	94% (74%–99%)
		R2	15	2	3	83% (60%–94%)
	1/10th SD, 100Sn kVp, ADMIRE 3	R1	17	1	1	94% (74%–99%)
		R2	17	0	1	94% (74%–99%)
	1/10th SD, 150Sn kV, ADMIRE 3	R1	16	0	2	89% (67%–97%)
		R2	16	0	2	89% (67%–97%)
	1/10th SD, 70 kVp, ADMIRE 5	R1	17	0	1	94% (74%–99%)
		R2	16	0	2	89% (67%–97%)
	1/10th SD, 100Sn kVp, ADMIRE 5	R1	17	0	1	94% (74%–99%)
		R2	17	1	1	94% (74%–99%)
	1/10th SD, 150Sn kV, ADMIRE 5	R1	16	0	2	89% (67%–97%)
		R2	15	1	3	83% (60%–94%)
	1/20th SD, 70 kVp, ADMIRE 3	R1	16	3	2	89% (67%–97%)
		R2	16	1	2	89% (67%–97%)
	1/20th SD, 100Sn kVp, ADMIRE 3	R1	17	0	1	94% (74%–99%)
		R2	17	0	1	94% (74%–99%)
	1/20th SD, 150Sn kV, ADMIRE 3	R1	16	1	2	89% (67%–97%)
		R2	16	2	2	89% (67%–97%)
	1/20th SD, 70 kVp, ADMIRE 5	R1	16	4	2	89% (67%–97%)
		R2	16	3	2	89% (67%–97%)
	1/20th SD, 100Sn kVp, ADMIRE 5	R1	17	0	1	94% (74%–99%)
		R2	17	0	1	94% (74%–99%)
	1/20th SD, 150Sn kV, ADMIRE 5	R1	16	1	2	89% (67%–97%)
		R2	16	1	2	89% (67%–97%)

CT indicates computed tomography; TP, true-positive; FP, false-positive; FN, false-negative; CI, confidence interval; SD, standard radiation dose; FBP, filtered back projection; SAFIRE, sinogram-affirmed iterative reconstruction; ADMIRE, advanced model-based iterative reconstruction.

Image Noise

Noise was highest in the images from second-generation dual-source CT at 120 kVp and lowest possible mAs and reconstructed with FBP (Table 2).

At the standard dose level, images at a tube voltage of 150 kVp Sn were associated with lower noise when compared with 70 kVp with both ADMIRE 3 and 5 (Table 2). In distinction, at the 1/10th and 1/20th dose levels, the data set acquired with 100Sn kVp showed the lowest noise level for both ADMIRE 3 ($P < 0.01$) and ADMIRE 5 ($P < 0.05$) (Fig. 4).

Accuracy of Lung Nodule Detection

The sensitivity for the detection of pulmonary nodules is summarized in Table 3. Sensitivity of pulmonary nodule detection was lowest in the images acquired with the second-generation dual-source CT at 120 kVp and lowest possible dose with both FBP and SAFIRE. In general, protocols at the 1/10th and 1/20th of standard dose had a similar or lower sensitivity as compared with standard dose protocols. Images at a tube voltage of 100Sn kVp (both ADMIRE 3 and 5) showed the highest sensitivity for pulmonary nodule detection at the 1/10th and 1/20th of standard dose levels (Table 3).

The highest numbers of false-positive (FP) ratings of pulmonary nodules occurred in image data acquired with second-generation dual-source CT and reconstructed with FBP and SAFIRE, ranging from 12 to 15. Lowest numbers of FP ratings were found in the 1/10th and 1/20th dose data sets acquired with third-generation dual-source CT at 100Sn kVp and reconstructed with ADMIRE strength levels 3 and 5 (total of 1 and 0 FP, respectively) (Table 3).

Diagnostic Confidence of Lung Nodule Detection

The interobserver agreement for diagnostic confidence ranged from substantial for the 120 kVp dose data set reconstructed with FBP (ICC = 0.68) to excellent for 70 kVp at standard dose reconstructed with ADMIRE 5 (ICC = 0.98).

The diagnostic confidence of pulmonary nodule detection was lowest in images acquired with second-generation dual-source CT at 120 kVp and lowest mAs and reconstructed with both FBP and SAFIRE (Fig. 5). For both the 1/10th and 1/20th doses, the confidence of nodule detection was significantly higher in images acquired at a tube voltage of 100Sn kVp as compared with 70 kVp and 150Sn kV for both ADMIRE 3 ($P < 0.05$) and ADMIRE 5 ($P < 0.01$). Compared with ADMIRE 3, ADMIRE 5 further improved the diagnostic confidence of nodule detection for all tube voltages, with this result being significant only at the tube voltage level of 150Sn kV ($P < 0.05$) at the 1/20th standard dose. In the standard dose level, diagnostic confidence was also higher with ADMIRE 5 as compared with 3; however, this did not reach statistical significance ($P > 0.05$). Representative image examples of the various protocols at the 1/20th dose level are provided in Figure 6.

Results from multivariate analysis indicated that radiation dose and reconstruction algorithm were significant (both $P < 0.001$) predictors of image noise, whereas the tube voltage setting was not ($P > 0.05$). Regarding the sensitivity, radiation dose represented a significant ($P < 0.05$) independent predictor (Table 4).

Patients

Representative image examples from the 2 patients scanned at the 1/10th and 1/20th dose, respectively, are provided in Figure 7. The images for patient 1 (lateral diameter at the level of the aortic root, 35 cm; anteroposterior diameter, 23 cm), scanned at the 1/10th standard dose ($CTDI_{vol}$, 0.30 mGy; DLP, 9 mGy cm; effective dose, 0.13 mSv), were assessed to be of diagnostic quality for image data sets reconstructed both with ADMIRE 3 (noise, 188 HU) and ADMIRE 5 (noise, 97 HU). Similarly, the images for patient 2 (lateral diameter, 29 cm; anteroposterior diameter, 20 cm), scanned at the 1/20th standard dose ($CTDI_{vol}$, 0.14 mGy; DLP, 5 mGy cm; effective dose, 0.07 mSv), were of diagnostic quality for image data sets reconstructed with both ADMIRE 3 (noise, 176 HU) and ADMIRE 5 (noise, 87 HU).

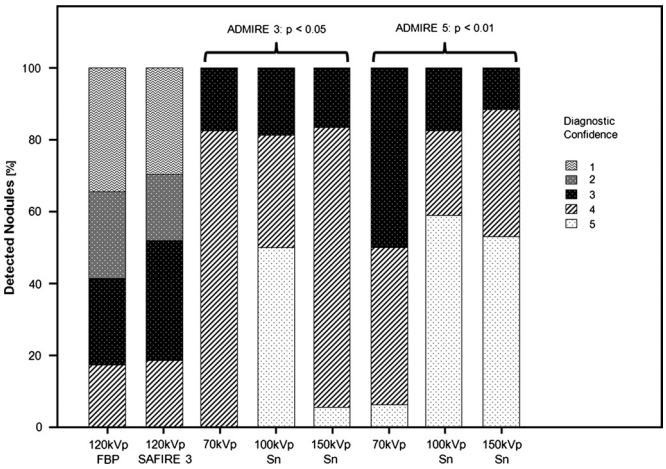

FIGURE 5. Diagnostic confidence distributions of 1 reader for protocols reconstructed with FBP, SAFIRE 3, and ADMIRE 3 and 5 (confidence score, 1 = unsure, 5 = high confidence). Use of 100Sn kVp was associated with the largest number of high diagnostic confidence ratings. Compared with ADMIRE 3, ADMIRE 5 further improved the diagnostic confidence. SD indicates standard dose.

DISCUSSION

This study sought to determine the value of single-energy imaging with spectral shaping for very low radiation dose CT of the chest using third-generation dual-source CT. For this purpose, we scanned a chest phantom containing solid nodules of various sizes at a random distribution starting with a low standard dose level of 1.3 mSv and then reducing doses further to 1/10th and 1/20th of the standard value, eventually resulting in an effective dose of 0.06 mSv. By doing so, our results indicate that image quality is maintained at this ultralow radiation dose, and the sensitivity and diagnostic confidence of pulmonary nodule detection are high when using a single-energy protocol at 100 kVp with tin filtration and when reconstructing images with ADMIRE. These ex vivo results were confirmed in 2 patients who were included in this study to demonstrate the feasibility of the protocol in vivo.

Optimizing the tube voltage to reduce patient dose while maintaining image quality represents a well-known technique and is established particularly for contrast-enhanced CT. Depending on the patient size, the dose efficiency typically improves when lowering the tube voltage. This is explained by the fact that the attenuation of iodine-based contrast agents increases at lower energy levels because the photoelectric effect is inversely proportional to the cube of the photon energy and proportional to the cube of the atomic number.

For noncontrast CT, this approach of decreasing the tube voltage is considered not beneficial. However, there is an optimal energy level for acquiring the data that allows for a reduction in the radiation dose to the patient. This principle is also known from dual-energy imaging, where it is used in 2 ways: an improved separation of the 2 energy spectra and dose-neutral scanning.[15] In this study, this approach was applied also for single-energy CT. By adding the TF, the shape of the energy spectra used for the acquisition is substantially narrowed, and less dose-efficient quanta are removed from the spectrum. This optimization approach finally allows for dose

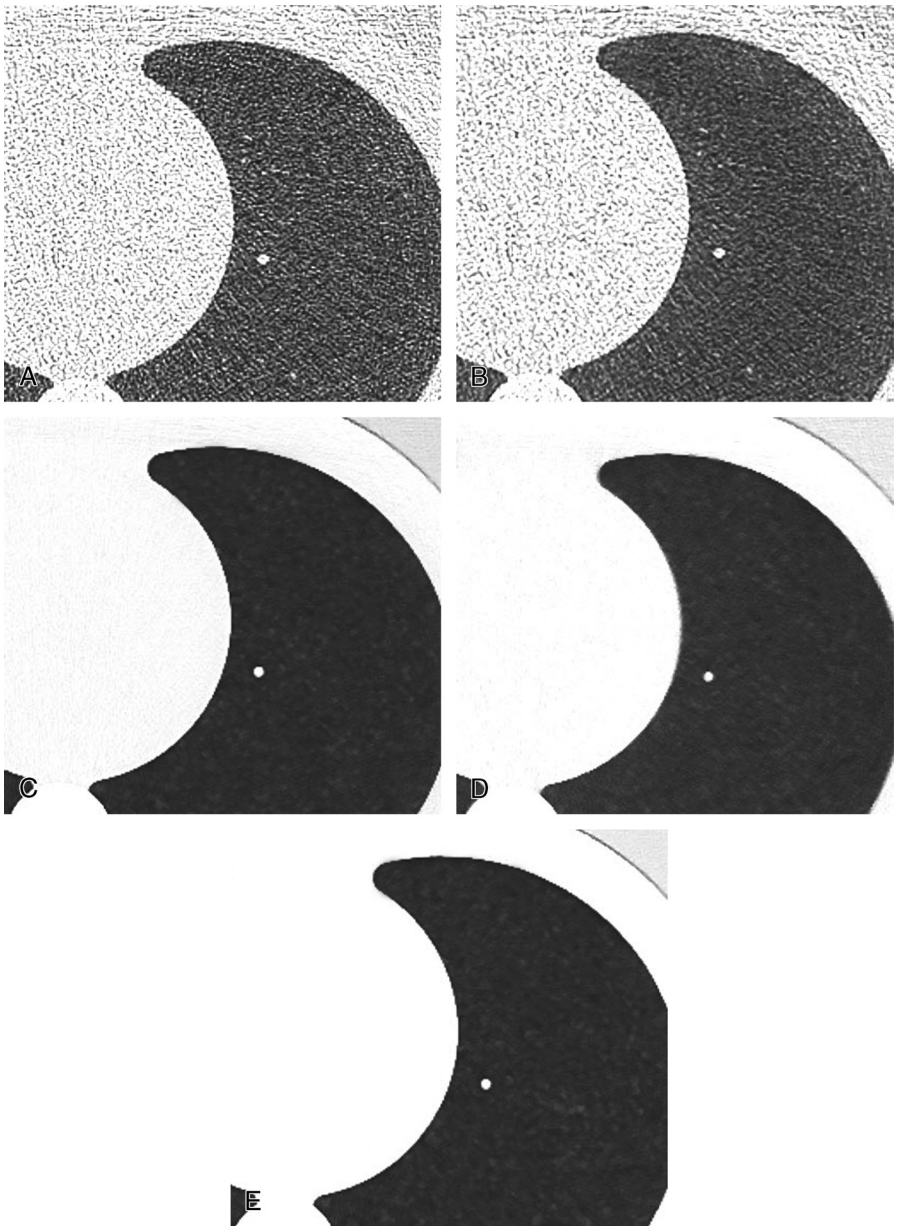

FIGURE 6. Representative transverse CT sections through the lung phantom with a pulmonary nodule in the left lung, scanned with second-generation dual-source CT at 120 kVp and 4 mAs ($CTDI_{vol}$, 0.28 mGy) (A) with FBP, (B) with SAFIRE strength level 3, and with third-generation dual-source CT ($CTDI_{vol}$, 0.15 mGy), (C) at 70 kVp and ADMIRE strength level 5, (D) at 100Sn kVp and ADMIRE strength level 5, and (E) 150Sn kV and ADMIRE strength level 5.

reduction. Both the 100 and 150Sn kV data sets had a lower noise than did the conventional spectral scan mode without TF at standard and 1/10th dose levels. The better dose performance of the 100Sn kVp compared with the 150Sn kV observed in the chest at the 1/10th and 1/20th dose levels can be explained by the comparatively small attenuation of the thorax due to the low attenuation of lung tissue. In areas of higher attenuation such as the abdomen pelvis, higher kVp values might be necessary, which will be the topic of future studies.

Based on our results, it seems that use of 70 kVp is of limited value for nonenhanced chest CT because noise, confidence, sensitivity, and the number of FP ratings of pulmonary nodules were higher as compared with those in the 100Sn kVp protocol. This could be explained by the fact that lung attenuation, although being lower than that of other body regions, is not low enough to allow sufficient penetration of low-energy photons through the lung tissue from a 70-kVp spectrum.

Several previous studies showed that the use of IR for chest CT allows for dose reduction without compromising diagnostic information.[9,10,23–28] Yamada et al[25] reported that, compared with FBP, model-based IR (GE Healthcare) enables significant reduction in image noise and artifacts and allows for a better detection of noncalcified pulmonary nodules on CT at 0.17 mSv using a tube voltage of 120 kVp and a tube current-time product of 4 mAs. Similar results with model-based IR and low-dose CT at 0.16 mSv were shown by Neroladaki et al[27] using a protocol with 100 kVp and 10 mA. Recently, Botelho et al[28] reported a high confidence for evaluating 5-mm ground-glass nodules in low-dose

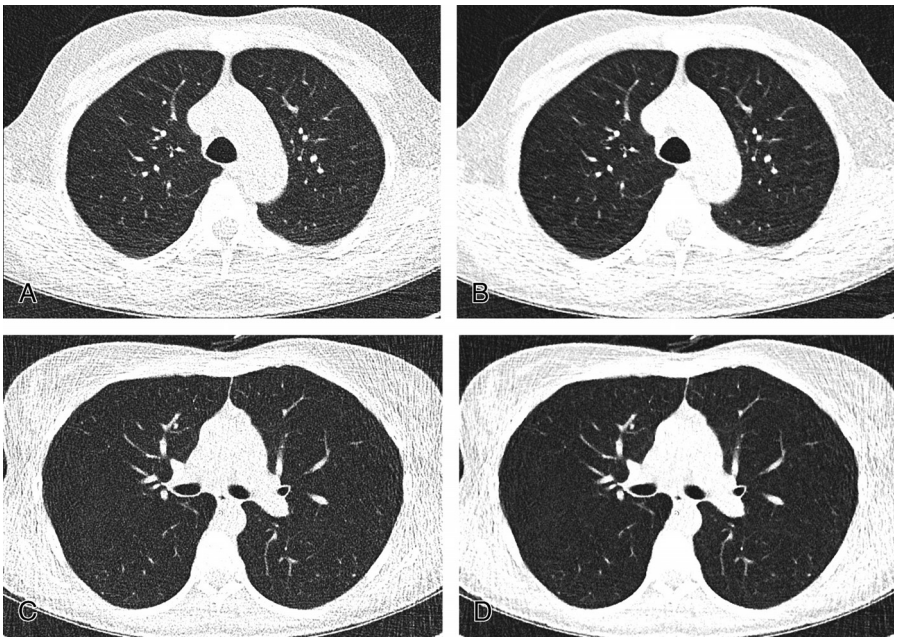

FIGURE 7. Representative transverse CT sections of a patient scanned at 1/10th dose (effective dose, 0.13 mSv) reconstructed with ADMIRE 3 (A) and ADMIRE 5 (B). Representative transverse CT sections from a patient scanned at 1/20th dose (effective dose, 0.07 mSv) reconstructed with ADMIRE 3 (C) and ADMIRE 5 (D).

chest CT at 0.41 to 0.24 mSv at a tube voltage of 100/120 kVp and a tube current-time product of 10 mAs and also for evaluating 12-mm ground-glass opacities at 0.24 to 0.11 mSv when using a protocol with 100/80 kVp and 10 mAs. Although these previous studies using different IR techniques and various tube voltage-tube current combinations gave rise to low-dose chest CT protocols at effective doses close to 0.1 mSv,[25–28] to the best of our knowledge, our study is the first showing the feasibility of lung CT at effective dose values as low as 0.06 mSv both ex vivo and in humans. When using a protocol with 100 kVp and spectral shaping by TF and reconstructing data with advanced IR, image quality was high and the sensitivity for detecting solid pulmonary nodules was excellent even at these ultralow dose levels.

In general, low radiation dose levels similar to those from conventional chest x-ray[29] are desired when it is intended to replace x-ray by CT for screening purposes. Regarding dose, the levels tested in this study for CT (0.06 mSv) are similar to those from a conventional chest x-ray study, which are reported to be in the range of 0.02 mSv for a posteroanterior study to 0.1 mSv for a posteroanterior and lateral study of the chest.[30] It is important to note that the images at this ultralow radiation dose level could not be obtained with second-generation dual-source CT at 120 kVp without spectral shaping, and images obtained at a higher radiation dose as compared with those from third-generation dual-source CT were considered of too low quality. In particular, the high image noise resulted in a high number of FP findings of pulmonary nodules, rendering the quality of images not sufficient.

Iterative reconstruction techniques have been introduced to the CT image reconstruction domain with the goal of reducing image noise in CT data acquired at lower radiation doses. First-generation IR techniques, such as IR in image space (Siemens), processed images in the image domain.[31] Pontana et al[9] reported improved conspicuity of ground-glass opacities, ill-defined micronodules, and emphysematous lesions with IR in image space (at settings 3 and 5) at 35% lower radiation doses compared with FBP. Being a second-generation IR technique, SAFIRE takes information from the raw data and processes data in the image domain.[32–34] Baumueller et al[13] showed that use of SAFIRE in low-dose lung CT reduces noise, improves image quality, and renders more studies diagnostic as compared with images reconstructed with FBP. Kalra et al[34] showed that use of SAFIRE allows for a reduction in radiation dose by approximately 65% without losing diagnostic information in lung CT. Our study was performed with a third-generation dual-source CT machine that includes a new generation of IR technique, that is, ADMIRE. This technique combines in an iterative approach statistical data modeling in the raw data domain and model-based noise detection in the image domain.

In our research, we showed that, at the same 1/20th dose level, use of ADMIRE 3 and 5 resulted in a mean of 27% and 63% reduction in image noise, respectively, compared with FBP. When compared with SAFIRE 3, ADMIRE 5 showed an image noise reduction of 50% at all 3 dose levels. Use of ADMIRE 5 also resulted in an improved subjective image quality at both the 1/10th and 1/20th dose levels as well as in a higher diagnostic confidence compared with ADMIRE 3.

Our study had some limitations. First, we have to acknowledge the inherent limitations of a phantom study. This holds particularly true for the homogenous background of the simulated lung parenchyma of our phantom. However, repetitive scanning with various CT protocols precludes application in humans for ethical reasons. Moreover, sensitivity studies on pulmonary nodule detection are limited in vivo because, usually, no gold standard is available. In addition, the feasibility of chest CT at this ultralow radiation dose level was demonstrated

TABLE 4. General Linear Model for the Prediction of Image Noise and Sensitivity

	Image Noise		Sensitivity	
	F	*P*	*F*	*P*
Radiation dose	33.6	<0.001	5.7	0.02
Tube voltage and tin filter	0.7	0.53	3.6	0.06
Reconstruction	37.7	<0.001	0.06	0.8

in vivo in 2 patients. Second, we did not apply other tube voltage settings, such as 80, 110, or 130 kVp, and did not compare images obtained with and without spectral shaping, although this is possible with third-generation dual-source CT. In addition, we did not reconstruct images with ADMIRE strength levels 1, 2, and 4. However, we included in our analysis a total of 18 data sets with representative tube voltage and IR settings. Third, we investigated protocols and reconstruction settings for solid but not for ground-glass or part-solid nodules.[35] Fourth, we did not test the intraobserver variability of readers for detecting pulmonary nodules. Finally, we used an anthropomorphic phantom of average adult size, and the optimal CT protocol and reconstruction settings in overweight and obese patients were not tested.

In conclusion, our study suggests that radiation dose levels of nonenhanced chest CT for the detection of pulmonary nodules can be lowered down to a level of 0.06 mSv when using single-energy scanning at 100 kVp with spectral shaping and when using advanced IR techniques while image quality remains diagnostic and sensitivity remains high. Future studies are needed to assess the value of this protocol in a large patient population.

REFERENCES

1. Bankier AA, Tack D. Dose reduction strategies for thoracic multidetector computed tomography: background, current issues, and recommendations. *J Thorac Imaging*. 2010;25:278–288.
2. Kalender WA, Buchenau S, Deak P, et al. Technical approaches to the optimisation of CT. *Phys Med*. 2008;24:71–79.
3. Christner JA, Zavaletta VA, Eusemann CD, et al. Dose reduction in helical CT: dynamically adjustable z-axis X-ray beam collimation. *AJR Am J Roentgenol*. 2010;194:W49–W55.
4. Baumueller S, Alkadhi H, Stolzmann P, et al. Computed tomography of the lung in the high-pitch mode: is breath holding still required? *Invest Radiol*. 2011;46:240–245.
5. Paul NS, Blobel J, Prezelj E, et al. The reduction of image noise and streak artifact in the thoracic inlet during low dose and ultra-low dose thoracic CT. *Phys Med Biol*. 2010;55:1363–1380.
6. Thibault JB, Sauer KD, Bouman CA, et al. A three-dimensional statistical approach to improved image quality for multislice helical CT. *Med Phys*. 2007; 34:4526–4544.
7. Kalra MK, Maher MM, Sahani DV, et al. Low-dose CT of the abdomen: evaluation of image improvement with use of noise reduction filters pilot study. *Radiology*. 2003;228:251–256.
8. Pontana F, Pagniez J, Flohr T, et al. Chest computed tomography using iterative reconstruction vs filtered back projection, part 1: evaluation of image noise reduction in 32 patients. *Eur Radiol*. 2011;21:627–635.
9. Pontana F, Duhamel A, Pagniez J, et al. Chest computed tomography using iterative reconstruction vs filtered back projection, part 2: image quality of low-dose CT examinations in 80 patients. *Eur Radiol*. 2011;21:636–643.
10. Prakash P, Kalra MK, Ackman JB, et al. Diffuse lung disease: CT of the chest with adaptive statistical iterative reconstruction technique. *Radiology*. 2010; 256:261–269.
11. Yanagawa M, Honda O, Yoshida S, et al. Adaptive statistical iterative reconstruction technique for pulmonary CT: image quality of the cadaveric lung on standard- and reduced-dose CT. *Acad Radiol*. 2010;17:1259–1266.
12. Leipsic J, Nguyen G, Brown J, et al. A prospective evaluation of dose reduction and image quality in chest CT using adaptive statistical iterative reconstruction. *AJR Am J Roentgenol*. 2010;195:1095–1099.
13. Baumueller S, Winklehner A, Karlo C, et al. Low-dose CT of the lung: potential value of iterative reconstructions. *Eur Radiol*. 2012;22:2597–2606.
14. Aberle DR, Berg CD, Black WC, et al. The National Lung Screening Trial: overview and study design. *Radiology*. 2011;258:243–253.
15. Stolzmann P, Leschka S, Scheffel H, et al. Characterization of urinary stones with dual-energy CT: improved differentiation using a tin filter. *Invest Radiol*. 2010;45:1–6.
16. Morsbach F, Desbiolles L, Plass A, et al. Stenosis quantification in coronary CT angiography: impact of an integrated circuit detector with iterative reconstruction. *Invest Radiol*. 2013;48:32–40.
17. Clinthorne NH, Pan TS, Chiao PC, et al. Preconditioning methods for improved convergence rates in iterative reconstructions. *IEEE Trans Med Imaging*. 1993; 12:78–83.
18. Park M, Chung YE, Lee HS, et al. Intraindividual comparison of diagnostic performance in patients with hepatic metastasis of full-dose standard and half-dose iterative reconstructions with dual-source abdominal computed tomography. *Invest Radiol*. 2014;49:195–200.
19. Keat N. Comparison of assessment techniques for CT scanner spatial resolution measurement. Available at: http://www.ctug.org.uk/meet05-10-06/assessment_techniques_ct_spatial_resolution.pdf. Accessed October 2013.
20. Shrimpton P. *Assessment of patient dose in CT. NRPB-PE/1/2004*. Chilton, England: National Radiological Protection Board, 2004.
21. Fischbach F, Knollmann F, Griesshaber V, et al. Detection of pulmonary nodules by multislice computed tomography: improved detection rate with reduced slice thickness. *Eur Radiol*. 2003;13:2378–2383.
22. Landis JR, Koch GG. The measurement of observer agreement for categorical data. *Biometrics*. 1977;33:159–174.
23. Singh S, Kalra MK, Gilman MD, et al. Adaptive statistical iterative reconstruction technique for radiation dose reduction in chest CT: a pilot study. *Radiology*. 2011;259:565–573.
24. Desai GS, Uppot RN, Yu EW, et al. Impact of iterative reconstruction on image quality and radiation dose in multidetector CT of large body size adults. *Eur Radiol*. 2012;22:1631–1640.
25. Yamada Y, Jinzaki M, Tanami Y, et al. Model-based iterative reconstruction technique for ultralow-dose computed tomography of the lung: a pilot study. *Invest Radiol*. 2012;47:482–489.
26. Katsura M, Matsuda I, Akahane M, et al. Model-based iterative reconstruction technique for ultralow-dose chest CT: comparison of pulmonary nodule detectability with the adaptive statistical iterative reconstruction technique. *Invest Radiol*. 2013;48:206–212.
27. Neroladaki A, Botsikas D, Boudabbous S, et al. Computed tomography of the chest with model-based iterative reconstruction using a radiation exposure similar to chest X-ray examination: preliminary observations. *Eur Radiol*. 2013;23:360–366.
28. Botelho MP, Agrawal R, Gonzalez-Guindalini FD, et al. Effect of radiation dose and iterative reconstruction on lung lesion conspicuity at MDCT: does one size fit all? *Eur J Radiol*. 2013;82:e726–e733.
29. Lehnert T, Naguib NN, Wutzler S, et al. Comparative study between mobile computed radiography and mobile flat-panel radiography for bedside chest radiography: impact of an antiscatter grid on the visibility of selected diagnostically relevant structures. *Invest Radiol*. 2014;49:1–6.
30. Mettler FA Jr., Huda W, Yoshizumi TT, et al. Effective doses in radiology and diagnostic nuclear medicine: a catalog. *Radiology*. 2008;248:254–263.
31. Hu XH, Ding XF, Wu RZ, et al. Radiation dose of non-enhanced chest CT can be reduced 40% by using iterative reconstruction in image space. *Clin Radiol*. 2011;66:1023–1029.
32. Winklehner A, Karlo C, Puippe G, et al. Raw data-based iterative reconstruction in body CTA: evaluation of radiation dose saving potential. *Eur Radiol*. 2011;21:2521–2526.
33. Wang R, Schoepf UJ, Wu R, et al. Image quality and radiation dose of low dose coronary CT angiography in obese patients: sinogram affirmed iterative reconstruction versus filtered back projection. *Eur J Radiol*. 2012;81:3141–3145.
34. Kalra MK, Woisetschlager M, Dahlstrom N, et al. Sinogram-affirmed iterative reconstruction of low-dose chest CT: effect on image quality and radiation dose. *AJR Am J Roentgenol*. 2013;201:W235–W244.
35. Kim H, Park CM, Woo S, et al. Pure and part-solid pulmonary ground-glass nodules: measurement variability of volume and mass in nodules with a solid portion less than or equal to 5 mm. *Radiology*. 2013;269:585–593.